COMPARISON OF OPAQUE NODULES IN UOCS WATONGA AND SEMARKONA S. P. Alpert (salpert@amnh.org)[1], D. S. Ebel[1,2], and M. K. Weisberg[1,2,3]. [1]Dept. of Earth and Planetary Sci., American Muesum of Natural History, New York, NY, 10024, USA. [2]Earth and Environmental Sci., CUNY Graduate Center, New York, NY, 10016, USA. [3]Dept. Physical Sci., Kingsborough Community College, CUNY, Brooklyn, NY, 11235, USA.

Introduction: Opaque nodules (ONs), also referred to as metal sulfide nodules (MSNs), or historically as M-type (metallic) chondrules [13] represent a small portion of the total volume of most types of chondrites [1]. Despite their small volume, ONs may contain significant amounts of untapped information pertaining to the formation of metal in chondrites and to metal fractionation from silicates in the early Solar System. ONs have been described in EH3, EL3, ordinary, and CK chondrites [2-12]. Attempts have also been made at creating experimental analogues for sulfide assemblages under ambient pressure and high temperature [17].

Understanding the process of metal-silicate fractionation in the evolution of solids in the Solar System is key to understanding the formation and composition of the inner planets. Metal content is a key distinguishing factor between the ordinary chondrites, but detailed description of the similarities and differences in metal occurrence in chondrites of the same group is so far lacking. This study presents comparative analysis of the ONs in Semarkona (LL 3.00-3.01, fall) and Watonga (LL 3.05-3.1, find).

Methods: Element x-ray intensity maps were collected using the Cameca SX100 electron microprobe (EMP) at the AMNH for four polished sections of Semarkona [4128-t1-ps2a, 4128-5, 4128-t6-ps1a, 4128-t5-ps1a] and three sections of Watonga [LL3.05-3.1; wat-1, wat-2, wat-3]. Individual nodules were identified from the overview maps and re-mapped at 1 µm/pixel resolution, 15 ms dwell time, 40 nA beam current using two passes of five wavelength dispersive spectrometers (WDS: Mg, Ni, Ti, Al, Ca, and Si, Fe, Cr, P, S). A back-scattered electron (BSE) image was also taken of each nodule. Conditions were selected to maximize peak counts while optimizing acquisition time. Individual element maps were exported in gray-scale 32-bit files, mosaicked, and combined into color-balanced 24-bit three-element, red-green-blue (RGB) composite maps using custom software to colorize each pixel based on the intensity of the corresponding element (Fig. 1).

Quantitative point analysis using the EMP was conducted for Mg, Fe, Cr, Si, S, Na, Co, Ti, Al, P, Ni, Mn, and Ca at 20 nA and 15 kV, with a 1 µm spot size. Count times varied by element, ranging from 30 ms to 120 ms based on expected modal abundance of the analyte. Qualitative point analysis was also conducted on the Zeiss EVO60 VPSEM in the AMNH's Microscopy and Imaging Facility.

Modal abundances of mineral phases were determined using a modified version of the software tools described in [15]. Thresholds for each phase were identified in ImageJ based on linear combinations of the 32-bit raw .tif files.

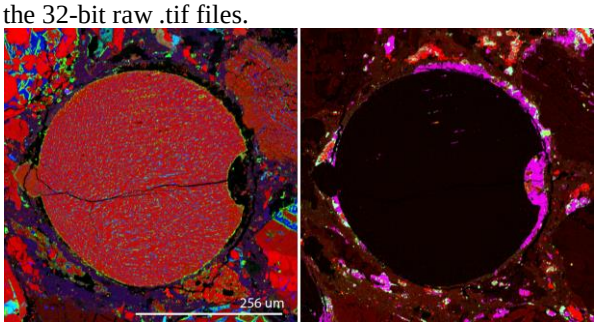

Figure 1 – ON rim on chondrule (sem-4128-5-chm5). RGB channels = MgCaAl (left) and FeNiS (right)

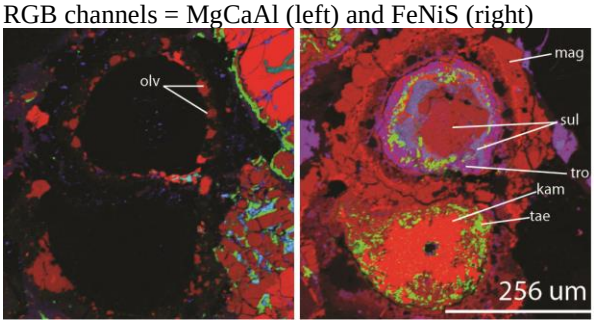

Figure 2 – paired ONs with layering. RGB channels = MgCaAl (left) and FeNiS (right)

Results: In both meteorites ONs are found in a spectrum of locations between interstitial to, and completely entrained in, chondrules. Interstitial ONs can be found conforming to the curvature of nearby chondrules and in some extreme cases apparently forming rims surrounding chondrules (Fig. 1). ONs frequently occur grouped together in pairs (Fig. 2), and in rare cases in Semarkona, clusters of three or more. ONs in both meteorites range in size from ~50 to 550 µm. Some ONs in both meteorites contain silicate inclusions (Fig. 3), or silicate rims.

Modal analysis reveals four primary phases, indicated in Fe-Ni-S RGB composite maps as: an Fe-oxide phase (dark red), an Fe-sulfide (purple-blue), Ni-rich metal (green) and Fe-rich metal (bright red).

Based on relative peak heights of oxygen in EDS analyses the Fe-oxide phase is likely magnetite [cf., 13]. WDS point analyses were conducted on the other phases to determine their compositions. Ni-rich metal contains: 35 wt% Fe, 64 wt% Ni, 0.7 Co and is likely taenite. Fe-rich metal contains 7-8 wt% Ni, with the remainder Fe and is likely kamacite. Sulfide phases

range from 20 to 35 wt% S; those on the higher end are probably troilite. Sulfide phases with low S generally exhibited low totals (74 – 96 wt%) and include Ni as high as 12 wt%. EDS analyses show oxygen peaks making up the difference.

Silicate phases are small (usually < 25 μm) and range in composition from olivine (Fig. 2, ~Fo_{93}), to a fine-grained silicate (Fig. 3) with Mg 7 wt%, Ca 5 wt%, Al 5 wt%, and Si 29 wt%, where Na may have migrated under the long (10ms) count time and high energy of the beam.

Modal analysis software output indicates that phases occur heterogeneously throughout ONs. Some ONs in Semarkona exhibit repeating layered structures with plessitic kamacite and taenite surrounded by layers of sulfide, oxide, and silicate [cf., 14].

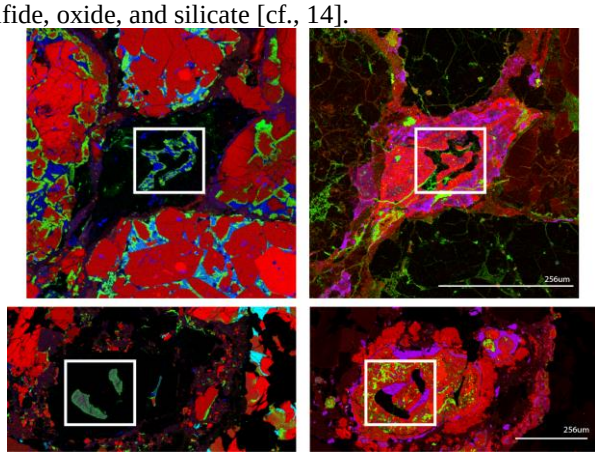

Figure 3 – Silicate inclusions (white boxes) in both wat-3-m8 (top) and sem-4128-t6-ps1a-m6 (bottom). RGB channels = MgCaAl (left column) and FeNiS (right column)

Discussion: Clusters of ONs with no matrix between them show similarities to the "cluster chondrules" described by [16]. These ONs could have been formed under similar conditions prior to final accretion on their parent body. From RGB maps we observe that three phases dominate the nodules: metal, oxide, and sulfide. Analysis of the ratio of total intensities of pixel values for S/Fe and Ni/Fe indicates discrete ratios of these elements in each ON, representing a mixing line of the dominant phases. Too few ONs have been analyzed to observe a trend in the ratios, however, with more statistics, S-rich and S-poor nodules should fall in a bimodal distribution of ratios.

Similar ratios in ONs in Watonga are more closely grouped, indicating more homogenized compositions. This is likely due to S and Ni (and P) mobilization during terrestrial alteration, as evidenced by the presence of Ni-, P-rich veins in Watonga that cross-cut both ONs and chondrules, indicating their post-accretion formation (Fig. 4). Image analysis also shows a greater abundance of Fe oxides in Watonga than Semarkona indicating that Ni (with P) from Ni-rich oxide phases in Watonga was the primary source for the Ni-, P-rich veins.

Conclusions and Outlook: ONs in Semarkona and Watonga share similar phases and textures. ONs in Semarkona exhibit a bimodal distribution with respect to S intensity, however, due to terrestrial alteration, ONs in Watonga do not. Therefore, despite its classification as a LL 3.1 meteorite, extreme discretion must be exercised when observing features in the ONs in Watonga.

Acknowledgements: This research is supported by the AMNH and NASA Emerging Worlds grant NNX16AD37G (DSE).

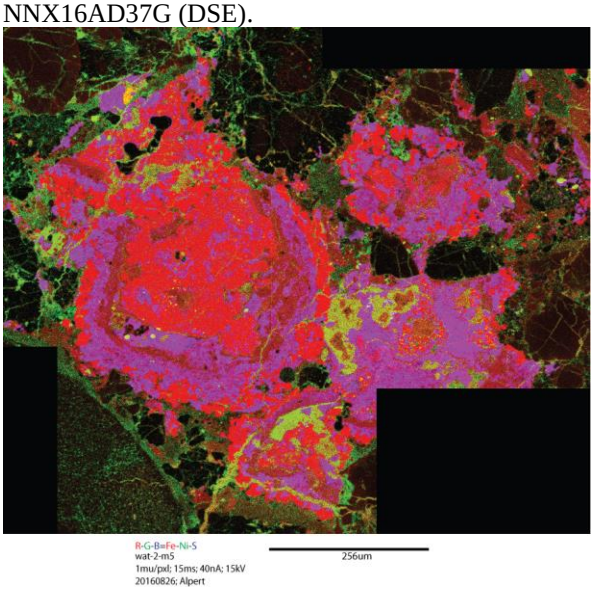

Figure 4 – Ni mobilization in Watonga meteorite.

References: [1] Ramdohr P. (1973) *The Opaque Minerals in Stony Meteorites*, Elsevier, 10-15. [2] Weisberg M. K. et al. (2006) *Meteorit. Planet. Sci. 69*, 5317. [3] Lehner S. W. et al. (2010) *Meteorit. Planet. Sci. 45*, 289–303. [4] Van Nierkirk D. and Keil K. (2011) *Meteorit. Planet. Sci. 46*, 1487–1494. [5] Horstmann M. et al. (2014) *Geochimica et Cosmochimica Acta 140*, 720–744. [6] Weisberg M. K. et al. (2013) *44th Lunar Planet. Sci, Conf. abstract* # 287. [7] Lin Y. et al. (2011) *42nd Lunar Planet. Sci, Conf. abstract* # 9040. [8] Scott E. R. D. (1973) *EOS 54*, 1125-1126. [9] Widom E. et al. (1986) *Geochimica et Cosmochimica Acta 50*, 1989–1995. [10] Kong P. et al. (1998) *Meteorit. Planet. Sci. 33*, 993–998. [11] Lauretta D. S. and Buseck P. R. (2003) *Meteorit. Planet. Sci. 38*, 59-79. [12] Rubin A. E. (1993) *Meteoritics 28*, 130-135. [13] Gooding J. L. and Keil K. (1981) *Meteoritics, 16, 1*, 24. [14] Grossman J. N. and Wasson J. T. (1985) *Geochem. et Cosmochim. Acta, 49*, 925-939. [15] Ebel D.S. et al. *Geochimica et Cosmochimica Acta 172*, 322-356. [16] Metzler K. (2012) *Meteorit. Planet. Sci. 47*, 2193-2217. [17] Schrader D. L. and Lauretta D. S. (2010) *Geochimica et Cosmochimica Acta 74*, 1719-1733.